Tribol Lett (2011) 44:19–30
DOI 10.1007/s11249-011-9822-6

ORIGINAL PAPER

Zinc Dialkyl Phosphate (ZP) as an Anti-Wear Additive: Comparison with ZDDP

Paule Njiwa · Clotilde Minfray · Thierry Le Mogne · Béatrice Vacher · Jean-Michel Martin · Shigeki Matsui · Masaru Mishina

Received: 21 February 2011 / Accepted: 1 July 2011 / Published online: 12 July 2011

Abstract In this study, we are interested in the anti-wear properties of zinc dialkyl phosphate additive (**ZP**) in comparison with 'classical' zinc dialkyldithiophosphate (**ZDDP**). Friction tests were performed on a reciprocating tribometer using both ball-on-flat and cylinder-on-flat configurations under a Hertzian contact pressure of 0.9 GPa. Experiments were carried out as a function of temperature (25 and 100 °C), sliding speed (25, 50 and 100 mm/s) and additives concentrations. Ball wear scar diameters as well as friction coefficient were measured. In order to better understand the anti-wear mechanisms of these additives, friction tests were followed by surface analyses such as AES (Auger Electron Spectroscopy) and XPS (X-Ray Photoelectron Spectroscopy). Transmission Electron Microscopy (TEM) observations of the **ZDDP** and **ZP** tribofilms were also carried out to visualise the generated layers. The anti-wear capability of **ZP** molecule is discussed.

Keywords Anti-wear additives · Boundary lubrication · Wear · AES · XPS · TEM (EDS)

1 Introduction

Zinc dialkyldithiophosphate (**ZDDP**) is a well-known additive used in lubricating oils because of its multifunctional anti-wear (AW), extreme pressure (EP) and antioxidant properties. Nowadays, the harmful effect of **ZDDP** molecule on catalytic converter limits its use as an anti-wear additive for Internal Combustion Engine (ICE) oil. New lubricants with good tribological performances, i.e., exhibiting low friction and low wear, are needed regarding environmental limitations (Norm euros VI). The idea is to reduce the levels of phosphorus and sulphur, specific elements contained in the **ZDDP** molecule, at the origin of the damage of catalytic converters.

Two options are currently investigated:

- the development of systems completely different from **ZDDP** molecules using for example nanoparticles [1, 2].
- the development of additives with chemical composition close to **ZDDP**. The objective is to have the best anti-wear protection while limiting the content in phosphorus and sulphur [3–6] in the molecule.

This work focuses on the second option. The understanding of **ZDDP** anti-wear mechanism is important before going further with modified molecules. A sum up of **ZDDP** tribochemistry of tribofilm generation is so reported in the following.

The literature provides three main mechanisms explaining the decomposition of **ZDDP** additive molecule within the lubricant under test conditions. This degradation can be thermal [7–9], hydrolytic [10] or oxidative [11] thanks to hydroperoxides and peroxidic radicals present in the lubricant. Martin [12] estimates that the decomposition of **ZDDP** is mainly thermo oxidative when temperature exceeds 100 °C.

During this degradation process, **ZDDP** molecules and their decomposition products are adsorbed physically or chemically on metal surfaces. The deposited film is called

P. Njiwa (✉) · C. Minfray · T. Le Mogne · B. Vacher · J.-M. Martin
Université de Lyon, Ecole Centrale de Lyon, LTDS, UMR5513, Ecully, France
e-mail: paule.njiwa@ec-lyon.fr

S. Matsui · M. Mishina
JX Nippon Oil & Energy Corporation, Lubricant Research Laboratory, Tokyo, Japan

'thermal film', and it is further modified under rubbing conditions to generate a protective layer called 'tribofilm'.

Basically, **ZDDP** anti-wear additive decreases the wear in a contact running under mixed or boundary lubrication conditions thanks to this tribofilm generation (50–100 nm thick) on rubbing surfaces [13–15]. Surface analyses such as the X-ray Photoelectron Spectroscopy (XPS) showed that the bulk **ZDDP** tribofilms are mainly composed of a mixed zinc and iron short chain (ortho or pyro) phosphate glass with iron sulphides precipitates [16, 17]. The phosphate chains are longer [17–19] on the top of the tribofilm than in its bulk [20]. Recently, Zhou et al. [21] assumed the presence of ultrapolyphosphate in the outer layer. The **ZDDP** thermal films have similar composition to **ZDDP** tribofilms, but consisting mainly of a thinner outer layer of polyphosphate ($\approx$10 nm thick) grading to pyro- or orthophosphate in the bulk [7].

The structural evolution of tribofilm material (i.e. zinc polyphosphate) during tribological solicitation is important to clarify for a better understanding of **ZDDP** anti-wear mechanism. To investigate structural modification of the material thanks to the effect of hydrostatic pressure, zinc polyphosphate was compressed in Diamond Anvil Cell coupled with in situ Raman or EXAFS analyses [22, 23]. Simulations by quantum chemistry were also carried out [24]. Results suggest a change of coordination number of metallic cation and no polymerisation of phosphate chains. The effect of phosphate glass parameters on their mechanical properties (influence of metallic cations nature, presence of hydroxyl group on phosphate molecules etc…) was also investigated [25, 26].

To insure a strong adhesion of the tribofilm to the substrate and to 'digest' iron oxide wear particles, a tribochemical mechanism was reported in literature [12] proposing a reaction between zinc metaphosphate (representative of the top of the thermal film) and iron oxide (representative of the native iron oxide layer). During this reaction, a shortening of phosphate chain length is proposed and was confirmed by friction test on metaphosphate glass [27].

Recent studies [5, 28] showed that the use of zinc orthophosphate powders (crystalline grains of a few microns diameter) is an interesting alternative for anti-wear organic additives. Moreover, this material is free from sulphur and is very close in composition to the main part of the final **ZDDP** tribofilm. Furthermore, it was showed that the use of zinc orthophosphate powders as an anti-wear additive has the advantage of being effective at the first cycles of friction and at 25 °C [5].

In our study, the additive is close to zinc orthophosphate powder in terms of chemical composition and it has the advantage of being soluble in the base oil thanks to alkyl groups in the molecule. Then, the use of zinc phosphate additive (**ZP**) is expected to facilitate the formation of a phosphate base tribofilm even at 'low' temperature and low concentration because it can avoid the detrimental induction period. Actually, the thermal degradation, which is necessary for the activation of **ZDDP** molecule through the generation of degradation products, is not necessary using directly **ZP** additive since it is already the final tribofilm material which is directly introduced in the contact.

The aim of this work is so to compare the anti-wear property of **ZP** additive in comparison with zinc dithiophosphate (**ZDDP**).

The first part will relate to the comparison of the anti-wear behaviour of these two molecules at 25 and 100 °C. The second part will deal with the effect of the sliding speed on wear at 25 °C. Finally, a study of the behaviour of **ZP** tribochemical reaction will be carried out by coupling friction tests with surfaces analyses (AES) at different experiment durations. The role of the concentration is investigated.

2 Materials and Methods

2.1 Lubricants

Three lubricants were tested:

- A mineral base oil of group III noted **BO** in the following.
- A mixture of mineral base oil **BO** and zinc di-2-ethylhexyl dithiophosphate additive (containing 800 ppm of phosphorus) noted **ZDDP** in the following (Fig. 1a).
- A mixture of mineral base oil **BO** and zinc di-2-ethylhexyl orthophosphate (containing 800 ppm of phosphorus) noted **ZP** in the following (Fig. 1b). It is reminded that the **ZP** molecule does not contain any sulphur.

2.2 Materials

The balls used were 12.7 mm in radius and 30 nm (Ra_B) in roughness. The cylinders employed were 6 mm in length and 6 mm in diameter. The rectangular flats measured 10 × 8 × 2 mm^3. All these specimens are made of AISI 52100 steel. This iron alloy contains 97 wt% of Fe, 1.45

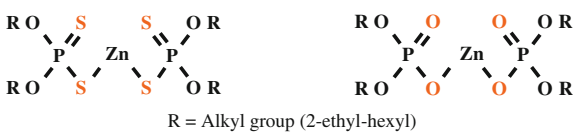

(a) Zinc dialkyl dithiophosphate (**ZDDP**) **(b)** Zinc dialkyl phosphate (**ZP**)

Fig. 1 **ZDDP** and **ZP** molecules

wt% of Cr, 1.04 wt% of C, 0.35 wt% of Mn and 0.23 wt% of Si. The cylinder and flat specimens were polished using diamond slurry with, respectively, 3 and 1 μm grains. The roughness after polishing of cylinder (Ra_C) and flat (Ra_F) are, respectively, 50 and 12 nm.

2.3 Methods

2.3.1 Tribological Parameters

Friction experiments were carried out using a home-made reciprocating cylinder (or ball)-on-flat tribometer [29]. First, experiments were performed in the ball-on-flat configuration to characterise wear behaviour of lubricants. Second, the cylinder-on-flat configuration was used to perform XPS surface analyses because the wear track is larger than the size of the XPS probe. The tribofilms generated under cylinder-on-flat configuration were homogeneous all over the track and of same morphology (patchy) as tribofilms generated under ball-on-flat configuration. It was so considered that tribofilms obtained in both cases were similar in composition (confirmed by XPS analyses not shown here) and morphology. Because the perfect alignment of a cylinder on a flat is difficult, ball-on-flat configuration was more convenient for wear measurements.

The influence of temperature and sliding speed on tribofilm formation was investigated. We choose temperatures similar to those encountered in an Internal Combustion Engine such as starting in ambient condition (25 °C) and in steady-state operation (100 °C).

The ball slides reciprocally on a fixed flat with a frequency of 7 Hz and a stroke length of 7 mm. The applied load for each test is 50 N corresponding to a maximum Hertzian pressure of 928 MPa. For the cylinder-on-flat test, the load was adjusted to obtain the same maximum Hertzian pressure as for the ball-on-flat experiment. The tests were repeated at least twice for each lubricant. The friction coefficient was measured all over the test. In the following, the average of all friction coefficient values measured for one test is reported. Standard deviation is calculated from the different repeated test values. The wear scar diameter on the ball was measured by optical microscopy. The wear tracks obtained were homogenous. The EHL film thickness and lambda ratio are calculated using the Hamrock Dowson formula [30] regarding various sliding speeds and values are reported in Table 1.

Table 1 Physical properties and rheological parameters of the mineral base oil (BO) in different test conditions

Sliding speed (mm/s)	Mineral base oil group III Sulphur content: <0.03%w Viscosity index > 120 Density at 15 °C:0.835 g/cm^3			
	Temperature (°C)			
	25		100	
	Dynamic viscosity (Pa.s)			
	3.02. E-02		3.36.E-03	
	Film thickness: h[a] (nm)	λ[b]	h[a](nm)	λ[b]
25	17.6	0.4	4.05	0.09
50	32.6	0.75	7.48	0.17
100	51.5	1.18	11.8	0.27

[a] Film thickness: calculation carried out from Hamrock relation [30]

[b] Ratio between the lubricant film thickness and the composite surfaces roughnesses (α)

$\alpha = \sqrt{(Ra_B^2 + Ra_F^2)}$ Ball ($Ra_B = 30$ nm) and Flat ($Ra_F = 12$ nm)

2.3.2 Surface Analyses

Before any analyse, samples were degreased by rinsing in n-heptane several times in ultrasonic bath.

The tribofilms formed on the flat (using the cylinder-on-flat configuration) were analysed by Auger Electron Spectroscopy (AES) and X-Ray Photoelectron spectroscopy (XPS). Surface analyses were performed under a pressure of 10^{-7} Pa in the analytical chamber. These techniques provide very surface sensitive information. The depth sensibility is different from one element to another but it is considered to be less than or equal to 10 nm.

The AES analyses were performed using a FEG electron gun 1000 (Thermo Scientific) −5 keV. The electron spot size is about 1 μm, and the lateral resolution is also about 1 μm. For XPS analyses, a monochromator X-ray AlKα source was used. The X-ray probe size (rectangular) is around 1300 μm^2. The emission angle is 90° with respect to the horizontal of the sample. The detection is made by the ESCALAB 220i (Thermo Scientific) spectrometer. The spectrometer is calibrated in energy to the 4f7/2 electronic level of gold (Binding energy: 84.0 eV). In a typical XPS analysis, a survey scan is carried out first in order to identify the different elements present in the sample. Then, high-resolution spectra of selected peaks (characteristics of each element) are performed. The deconvolution of these peaks allowed an identification of the different chemical species. Acquisition conditions for the survey spectra were as the following: pass energy of 100 eV, dwell time of 500 ms and step size of 1.0 eV. Concerning acquisition parameters for high-resolution spectra, they were slightly different: pass energy of 20 eV, dwell time of 500 ms and step size of 0.1 eV. The binding energy of carbon (C1s ~ at 284.8 eV) is used as a reference for any charge correction.

Special attention has been paid for fitting P_{2p}, S_{2p} (for **ZDDP**), O_{1s}, Fe_{2p3} and $Zn_{2p3/2}$ photopeaks. CasaXPS [31] software was used for performing the curve fitting procedures on AES and XPS spectra. For XPS, a Shirley background was used and the Lorentzian/Gaussian ratio (L/G) was fixed at 60%.

2.3.3 *Transmission Electron Microscopy (TEM)*

We used a JEOL 2010F TEM operating with 200 kV accelerating voltage and equipped with an Energy Dispersive X-ray spectrometer (EDX). The cross sections of the near-surface regions of the flat were obtained by the Focused Ion Beam (FIB) method. Before milling, platinum and tungsten layers were deposited on the worn track to preserve the surface from damage due to nano-machining with Ga^+ ion beam.

3 Results

3.1 Friction and Wear

First, let us examine the friction and anti-wear performances at low temperature (25 °C). The average friction coefficients measured during tests with **ZDDP** and **ZP** lubricants at 25 °C are shown in Table 2. Figure 2 illustrates the curve of friction coefficient versus time for the three different lubricants (**BO**, **ZDDP** and **ZP**) at 25 °C and 100 mm/s.

Wear scar diameters were measured on the balls for the three lubricants: **BO**, **ZDDP** and **ZP**, and the tests were carried out at 25 °C (room temperature) with sliding speeds of 100, 50 and 25 mm/s, respectively.

At 25 °C and 100 mm/s, friction coefficient (Table 2) obtained with **ZDDP** lubricant (0.119 ± 0.001) is approximately equal to the one obtained with **ZP** lubricant (0.117 ± 0.001). Concerning the anti-wear efficiency at 100 mm/s, Fig. 3 and Table 3 show the ball wear track diameters obtained after ball-on-flat test. As we can see, at room temperature, there is no significant difference between the anti-wear properties for the three lubricants. This is attributed to a predominant EHL/mixed lubrication regime at this temperature (see elevated film thickness and lambda ratio in Table 1). To increase contact severity, we divided the sliding speed by two (50 mm/s) but the sliding distance (360 m) was kept the same as for the experiment

Table 2 Friction coefficient for both the lubricant (**ZDDP** and **ZP**) at 25 and 100 °C with sliding speed of 25 and 100 mm/s

	Friction coefficient		
Temperature (°C)	25		100
Sliding speed (mm/s)	25	100	100
Lubricants			
BO	0.138 ± 0.000	0.095 ± 0.005	0.16 ± 0.02
ZP	0.116 ± 0.006	0.117 ± 0.001	0.105 ± 0.004
ZDDP	0.121 ± 0.002	0.119 ± 0.000	0.085 ± 0.009

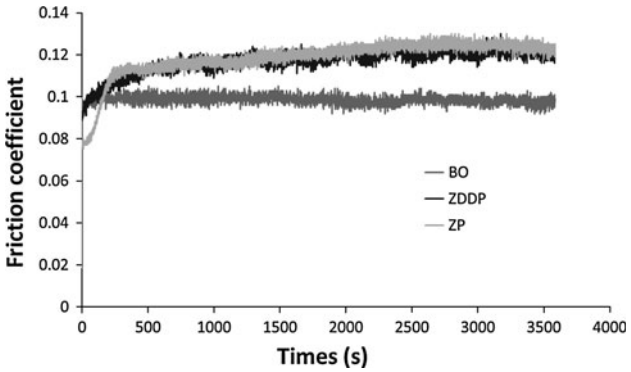

Fig. 2 Friction coefficient *curves* as a function of time at 25 °C with sliding speed of 100 mm/s under 0.9 GPa of Hertzian pressure for **BO**, **ZDDP** and **ZP** lubricants

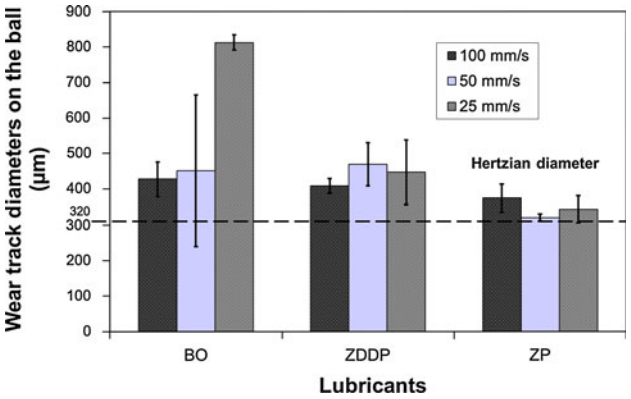

Fig. 3 Ball wear track diameters after ball-on-flat tests at 25 °C with sliding speed of 25, 50 and 100 mm/s under 0.9 GPa of Hertzian maximum pressure for lubricants **BO**, **ZDDP** and **ZP**

Table 3 Ball wear track diameters after ball-on-flat test at 25 °C with sliding speed of 25, 50 and 100 mm/s under 0.9 GPa of Hertzian maximum pressure for lubricants **BO**, **ZDDP** and **ZP**

	Wear track diameter on the ball (µm)		
	Temperature (25° C)		
Sliding speed (mm/s)	100	50	25
Lubricants			
BO	428 ± 48	452 ± 213	813 ± 22
ZDDP	409 ± 21	407 ± 61	448 ± 90
ZP	375 ± 39	321 ± 10	344 ± 38

at 100 mm/s. Figure 3 and Table 3 also present the wear results obtained at 50 mm/s. They indicate a slightly better anti-wear effect for **ZP** lubricant. We further increased the severity by using a sliding speed of 25 mm/s (always with the same sliding distance of the ball). Figure 3 and Table 3 illustrate too the wear results obtained for **ZDDP** and **ZP** lubricants at 25 °C and 25 mm/s. It can be noticed that wear is much higher with **BO** (813 ± 22 μm) than with **ZDDP** (448 ± 90 μm) and **ZP** (344 ± 38 μm) lubricants due to the occurrence of the boundary regime. Concerning the friction, there is no noticeable difference in friction coefficient (∼0.12) between **ZDDP** and **ZP** lubricants. However, this small sliding speed allowed us to discriminate clearly anti-wear performances with the **ZDDP** and **ZP** additives at room temperature. The overall results indicate a much better anti-wear performance for the **ZP** lubricant at low temperature and low speed in the boundary regime. Furthermore, optical observations of flat wear tracks for **ZDDP** and **ZP** lubricants (25 mm/s—25 °C) presented in Fig. 4 suggest also a better anti-wear behaviour of **ZP** additive as the number of tribofilm pads is higher for **ZP** than for **ZDDP** lubricant.

At 100 °C and 100 mm/s of sliding speed, compared with **BO** (685 ± 168 μm), wear on the balls for **ZDDP** (342 ± 8 μm) and **ZP** (418 ± 59 μm) lubricants drastically decreases (Table 4). The friction coefficients obtained with the three lubricants are summarised in Table 2. The optical images of flat wear tracks obtained with **ZDDP** and **ZP** lubricants at 100 mm/s are represented in Fig. 4. They show the presence of coloured patchy tribofilms typical of anti-wear action of this kind of P-containing additives.

Table 4 Ball wear track diameters after ball-on-flat tests at 100 °C with sliding speed of 100 mm/s under 0.9 GPa of Hertzian maximum pressure for lubricants **BO**, **ZDDP** and **ZP**

Lubricants	Wear track diameter on the ball (μm) Temperature (100 °C) Sliding speed (100 mm/s)
BO	685 ± 168
ZDDP	342 ± 8
ZP	418 ± 59

Looking at calculated EHL film thickness (11.8 nm) and lambda ratio (0.27) at 100 °C, we can assume that the lubrication regime at 100 mm/s sliding speed is predominantly boundary. The anti-wear performances of **ZP** (418 ± 59 μm) and **ZDDP** (342 ± 8 μm) lubricants are close, although **ZDDP** molecule exhibits a slightly better anti-wear behaviour Fig. 5.

3.2 AES and XPS Analyses

Let us examine surface chemistry of tribofilm at low temperature (25 °C) and low sliding speed (25 mm/s) where **ZP** was found much better than **ZDDP** (Fig. 3). Phosphorus, sulphur (detected only for **ZDDP**) and zinc are found in AES spectra performed on **ZDDP** and **ZP** tribofilms (Fig. 6). Iron is detected in the case of **ZDDP** only. Oxygen is mainly in oxide form (peak O_{KLL} ∼ 512 eV) in the **ZDDP** tribofilm and in a phosphate form (peak O_{KLL} ∼ 507 eV) for the **ZP** case. **ZDDP** tribofilm at room temperature consists of a mixture of zinc and iron

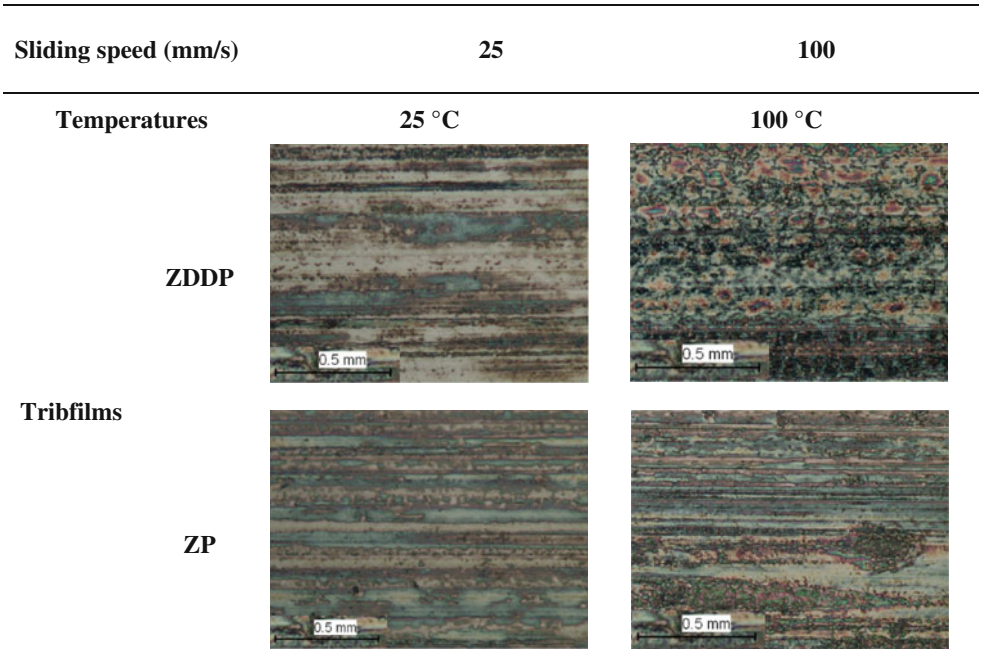

Fig. 4 Optical images of flat wear tracks (Ball-on-Flat configuration) obtained at 25 and 100 °C with sliding speed of 25 and 100 mm/s under 0.9 GPa of Hertzian maximum pressure with **ZDDP** and **ZP** lubricants

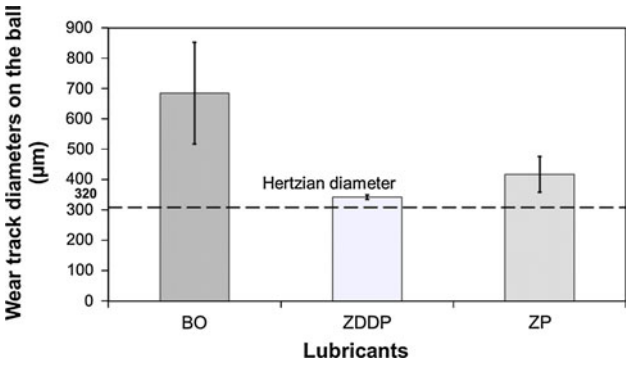

Fig. 5 Ball wear track diameters after ball-on-flat tests at 100 °C with sliding speed of 100 mm/s under 0.9 GPa of Hertzian maximum pressure for lubricants **BO**, **ZDDP** and **ZP**

phosphate with probably iron oxide and metallic sulphides [32]. On the other hand, the **ZP** tribofilm is made of zinc phosphate only.

XPS spectra carried out on **ZDDP** and **ZP** tribofilms obtained at room temperature and 25 mm/s (Fig. 7) also display phosphorus, sulphur (with **ZDDP**) and zinc. The O_{1s} peaks from **ZP** and **ZDDP** tribofilms show two contributions indicating that oxygen is involved mainly in phosphate form (531.6 eV (P–O) and 533.2 eV (P–O–P)) and another contribution is attributed to oxide form (529.6 eV) [17, 32]. However, this last contribution is found in very small amount and is negligible considering the fact that it is close to the detection limit.

Finally, the **ZDDP** and **ZP** tribofilms also consists mainly of a mixture of zinc and iron phosphate, with sulphide (162.3 eV) in case of **ZDDP** tribofilms. Iron oxide is also detected but AES and XPS results are not in total agreement in the case of **ZDDP** tribofilm. A strong iron oxide contribution was clearly found on the AES analysis but this was not so obvious on the XPS analyses. As the analysed area with AES technique ($\approx 1\ \mu m^2$) is much smaller than with XPS ($\approx 1300\ \mu m^2$), this difference is attributed to the local tribofilm heterogeneity.

Auger spectra of **ZDDP** and **ZP** tribofilms obtained at 100 mm/s and at 100 °C are shown in Fig. 8. The characteristic elements of the additives are detected in both **ZP** and **ZDDP** tribofilms: phosphorus, sulphur (detected only for **ZDDP**) and zinc. Oxygen is clearly in the phosphate chemical form (peak $O_{KLL} \sim 506$ eV). No iron is detected at the top of the two tribofilms. The results indicate that both **ZDDP** and **ZP** tribofilms are made of zinc phosphate (probably with some metallic sulphides for **ZDDP**).

XPS analyses were performed in the same tribofilm locations as for AES analyses. The advantage of XPS is to provide semi-quantitative elementary analysis. Figure 9 shows the general survey (SG) and O1s spectra of **ZDDP** and **ZP** tribofilms obtained at 100 °C and 100 mm/s. The O_{1s} peak from **ZDDP** tribofilm shows two contributions indicating that oxygen is involved mainly in phosphate form (531.6 eV (P–O) and 533.2 eV (P–O–P)) and another contribution attributed to oxide form (529.6 eV). However, this last contribution is found in very small amount (about 1.6 at % cf. Table 5) and is negligible considering the fact that it is close to the detection limit. Two small contributions of oxygen linked to carbon are also detected at 531.6 eV (C=O) and 533.2 (C–O) at same positions as phosphate peaks. Taking into account semi-quantification of corresponding carbon peak deconvolution, these two contributions are expected to be of few atomic percentages. The O_{1s} peak from **ZP** tribofilm shows the contributions of oxygen in phosphate form (531.6 eV (P–O) and 533.2 eV (P–O–P)) with no oxide form. S_{2p} binding energy from **ZDDP** additive corresponds to metallic sulphides (ZnS, FeS, FeS_2…) [16, 17] and is detected only in **ZDDP** tribofilm. The Table 5 shows the quantification of component detected on **ZDDP** and **ZP** tribofilms.

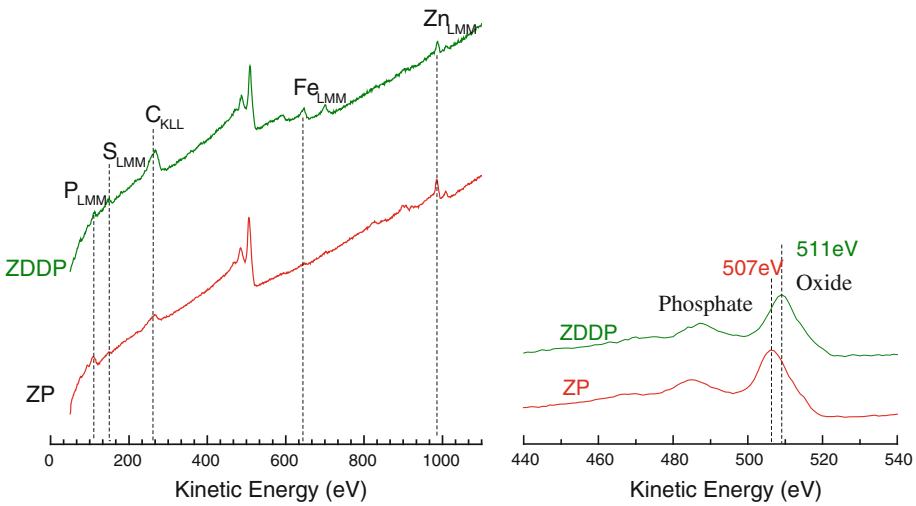

Fig. 6 Auger Spectra of **ZDDP** and **ZP** tribofilms obtained at 25 °C with a sliding speed of 25 mm/s under 0.9 GPa of Hertzian maximum pressure

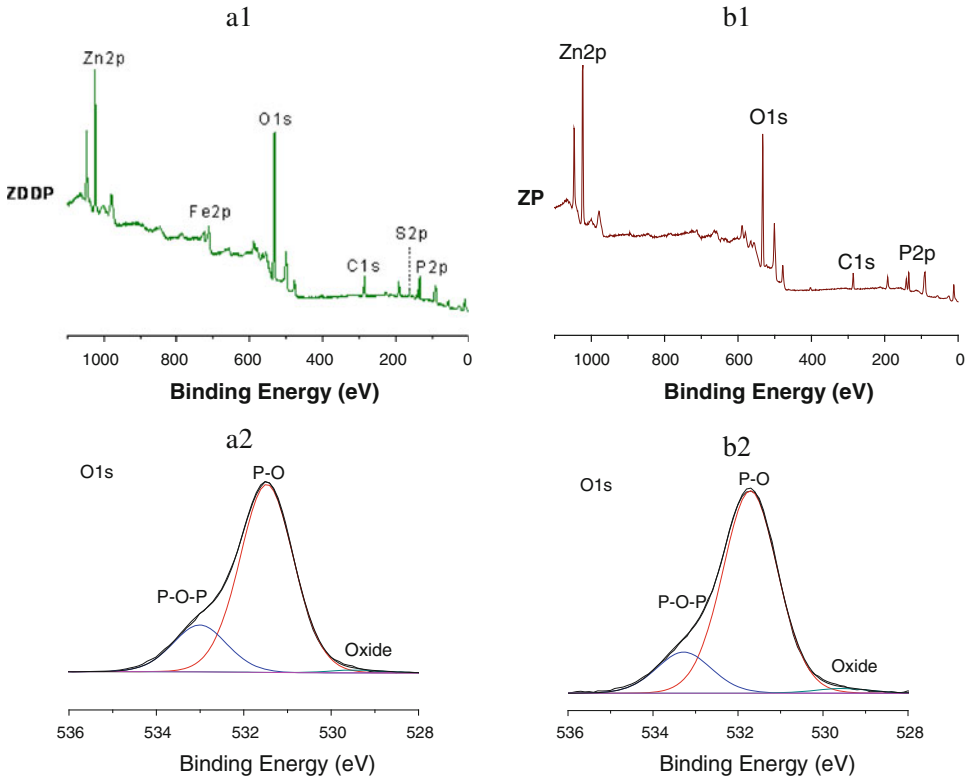

(a) XPS spectra: SG (a1) and O1s (a2) of **ZDDP** **(b)** XPS spectra: SG (a1) and O1s (a2) of **ZP**

Fig. 7 XPS spectra of **ZDDP** and **ZP** tribofilms obtained at 25 °C with a sliding speed of 25 mm/s under 0.9 GPa of Hertzian maximum pressure

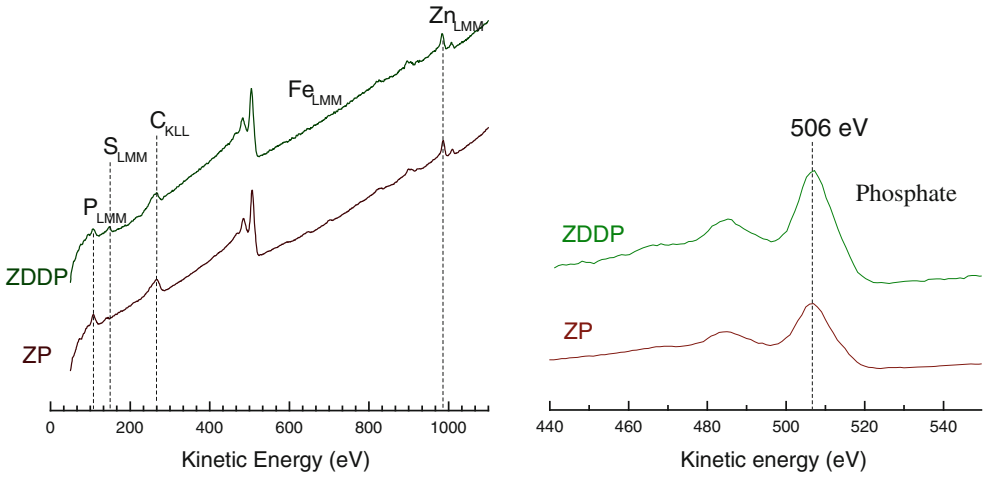

Fig. 8 Auger Spectra of **ZDDP** and **ZP** tribofilms obtained at 100 °C with a sliding speed of 100 mm/s under 0.9 GPa of Hertzian maximum pressure

The overall results of AES and XPS studies clearly show that **ZDDP** and **ZP** tribofilms formed at 100 °C and 100 mm/s consists of a zinc phosphate (with sulphide (162.3 eV) in the case of the **ZDDP**).

Figure 10 shows the TEM images of FIB cross sections for **ZDDP** and **ZP** tribofilms obtained at 100 °C and 100 mm/s. The tribofilms formed on steel is about 60 nm thick for both additives. The EDS spectra carried out on both **ZDDP** and **ZP** tribofilms confirm the elemental composition previously obtained by AES.

3.3 Wear Behaviour of ZDDP and ZP Molecule for Various Sliding Distances

Some additional tribological experiments (ball-on-flat) were performed at various sliding distance to study wear

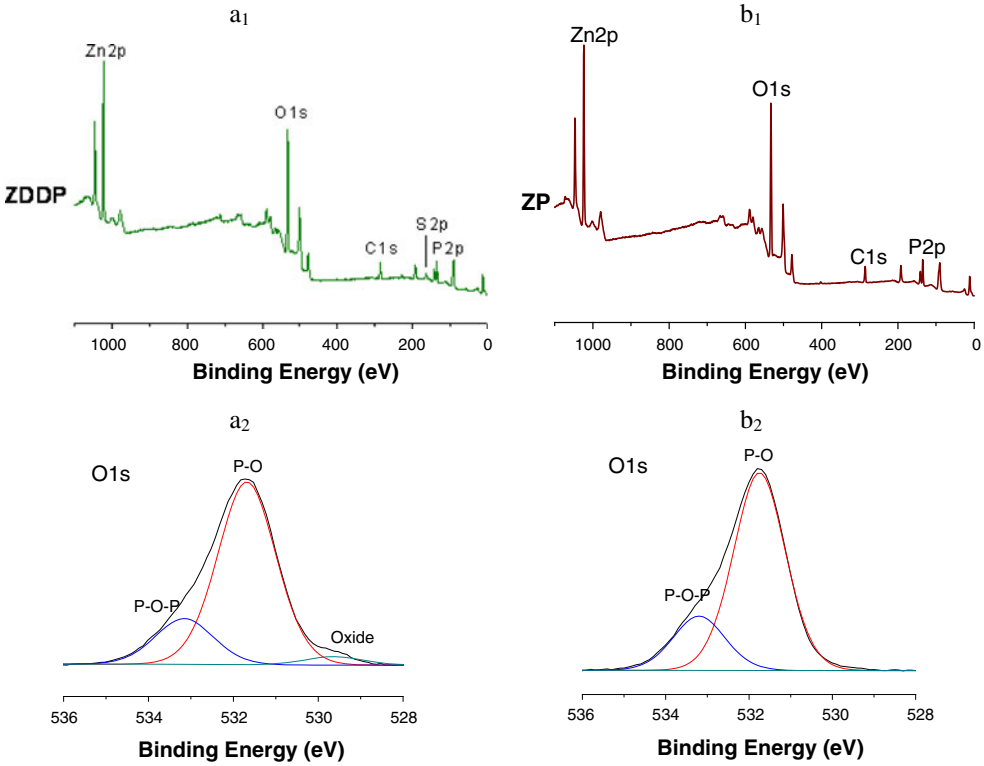

Fig. 9 XPS spectra of **ZDDP** and **ZP** tribofilms obtained at 100 °C with a sliding speed of 100 mm/s under 0.9 GPa of Hertzian maximum pressure

(a) XPS spectra: SG (a1) and O1 (a2) of **ZDDP**

(b) XPS spectra: SG (b1) and O1s (b2) spectrum of **ZP**

Table 5 XPS quantification (% at) of ZDDP and ZP tribofilms obtained at 100 °C with a sliding speed of 100 mm/s under 0.9 GPa of Hertzian maximum pressure

Name	Position (±0.2 eV)	FWHM	% at conc ZDDP tribofilm	% at conc ZP tribofilm
C1s (C–H)	284.8	1.3	10.7	9.1
C1s (C–O)	286.4		2.7	2.0
C1s (C=O)	288.5		1.0	0.6
O1s (P–O, C–O, C=O)	531.6	1.4	34.8	38.7
O1s (P–O–P)	533.2		8.7	10.6
O1s (oxide)	529.6		1.6	–
P2p3/2 (phosphate)	133.8	1.7	19.5	22.0
S2p3/2 (zinc, iron) sulphur	162.3	2.5	4.6	–
Zn2p3/2 (zinc phosphate)	1022.6	1.6	16.5	17.0

behaviour of **ZDDP** and **ZP** molecules during the tribofilm formation. The study was carried at 25 °C—25 mm/s (Fig. 11a) in the low-temperature regime where **ZP** was found more efficient and at 100 °C and 100 mm/s (Fig. 11b). Figure 11 presents wear results obtained at various sliding distance for the two additives at 25 °C—25 mm/s and at 100 °C—100 mm/s. Figure 11a presents wear results obtained at various test durations (4, 20, 120 and 240 min) corresponding, respectively, to different sliding distances (6, 30, 180 and 360 m) for the two additives at 25 °C and 25 mm/s. For **ZP** and **ZDDP** additives, the wear obtained at the beginning of the experiment (sliding distance = 6 m) is very small and close to the calculated Hertzian diameter. It is the same for **ZP** even after 360 m of sliding. However, for **ZDDP**, we observe a wear increase after 360 m of sliding. The Auger analyses of the wear scar show the presence of additive elements after 6 m of sliding in **ZDDP** and **ZP** tribofilms (Fig. 12), although iron is detected in each case. After 360 m of sliding, iron is detected in the **ZDDP** tribofilm but not for **ZP**. Moreover, friction tests were performed for 1–60 min at 100 mm/s of sliding speed and 100 °C. Experiment durations were adjusted in order to have same sliding distances (6 and 360 m) as for the experiment at

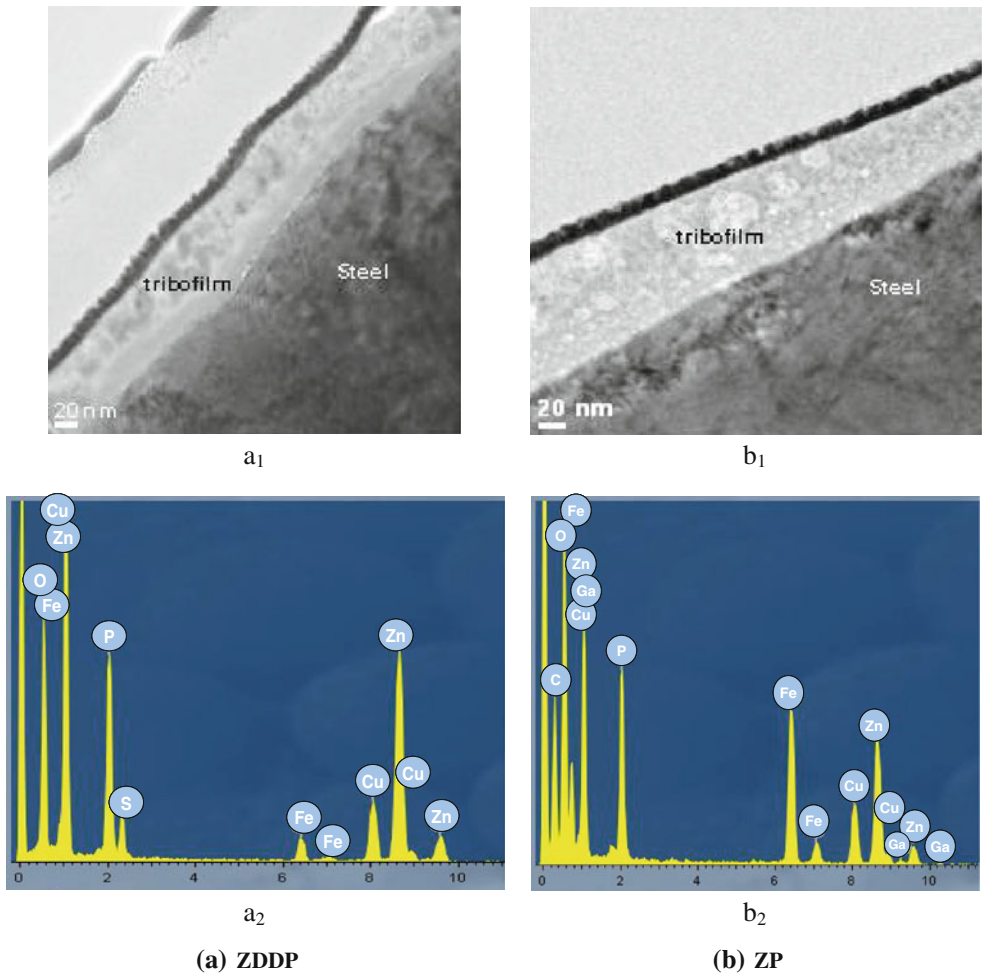

Fig. 10 TEM observations (a_1 et b_1) and EDX spectra (a_2 and b_2) of the FIB cross section of **ZDDP** (**a**) and **ZP** (**b**) tribofilms obtained at 100 °C with a sliding speed of 100 mm/s under 0.9 GPa of Hertzian maximum pressure

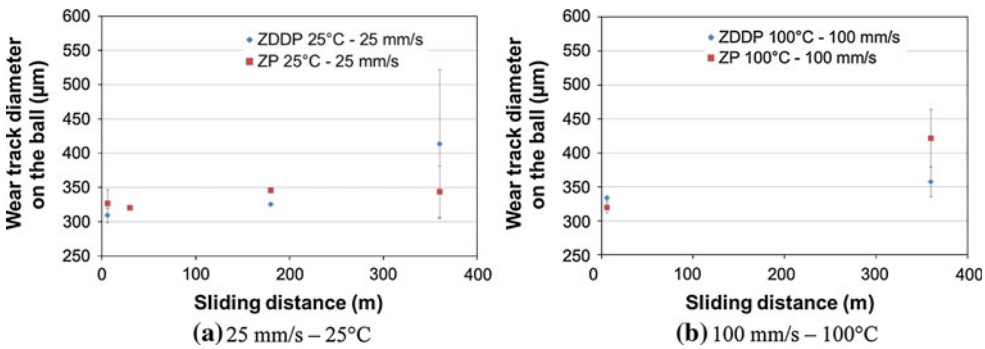

Fig. 11 Ball wear track diameters after ball-on-flat tests at 25 and 100 °C with different sliding distance for **ZDDP** and **ZP** lubricants

25 mm/s. For **ZP** and **ZDDP** additives, the wear obtained at the beginning of the experiment (sliding distance = 6 m) is small and close to Hertzian diameter. This wear increases slightly for **ZDDP** after 360 m of sliding. For **ZP** additives, same feature is found at the beginning of tests but wear is found to increase a little more after 360 m of sliding.

3.4 Effects of ZP and ZDDP Concentrations

We also focused on the effect of **ZDDP** and **ZP** concentrations on their anti-wear efficiency at room temperature and 25 mm/s of sliding speed for 240 min. Several dilutions were made by mixing a certain volume of base oil with a volume of **ZDDP** or **ZP** lubricants (25 and 75% of

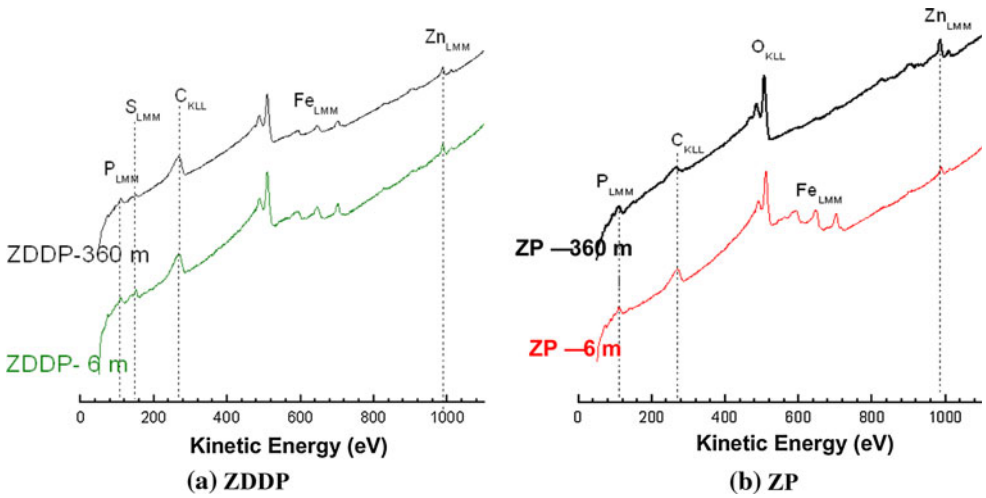

Fig. 12 Auger spectra obtained on **ZDDP** and **ZP** tribofilms after 6 and 360 m of sliding at 25 °C with a sliding speed of 25 mm/s under 0.9 GPa of Hertzian maximum pressure

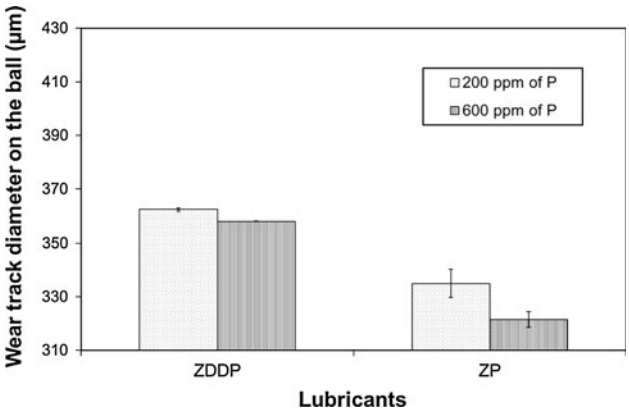

Fig. 13 Ball wear track diameters after ball-on-flat tests at 25 °C with sliding speed of 25 mm/s under 0.9 GPa of Hertzian maximum pressures for lubricant with different additives concentration (200 and 600 ppm of phosphorus)

base oil corresponding, respectively, to 600 and 200 ppm of P, respectively). Figure 13 shows wear scar diameters on balls at the three concentrations and at room temperature. As can be seen for the most dilute solution (75% **BO**—200 ppm of P), the wear scar diameter obtained with **ZDDP** lubricant ($\sim 358 \pm 0.1$ µm) is significantly higher than with **ZP** lubricant ($\sim 321 \pm 3.0$ µm). The comparison of **ZDDP** and **ZP** lubricants at low concentration gives evidence for the better anti-wear property of **ZP** at room temperature.

4 Discussion

At 100 °C and 100 mm/s for 60 min, both **ZP** and **ZDDP** molecules exhibit anti-wear capabilities (**ZDDP** molecule is slightly better) as well as similar tribofilms compositions. The absence of sulphur in **ZP** molecule does not inhibit the tribofilm formation. The origin of anti-wear capabilities of such phosphorus-based additives is probably the same for the two molecules. It is important to notice that we did not check the efficiency of these additives in the EP regime. Different mechanisms are proposed in literature related to specific tribochemical reaction pathways [12, 19] or specific tribofilm material modification under solicitations [24].

In the first case (tribochemical reactions), it is proposed that **ZDDP** molecule and its degradation products react under boundary conditions with native iron oxide of steel surfaces to form mixed zinc and iron phosphate glass [12]. Thanks to this tribochemical pathway, the tribofilm adheres well on metal surfaces. Additionally, any iron oxide particle trapped in the contact will lose its abrasive character when being digested in the phosphate tribofilm. In case of more severe lubrication conditions (extreme pressure), the tribofilm could not stay in the contact and a different tribochemical reaction occurs between iron metal and sulphur species. Metallic sulphides are generated in the contact. This last reaction is explaining the extreme pressure capabilities of **ZDDP** molecule.

Concerning the second mechanism at the origin of anti-wear capabilities of such material, it is related to interfacial material modification (zinc phosphate) under solicitations. A change of zinc atoms coordination number is proposed under hydrostatic pressure [24] and could so contribute to the modification of tribofilm mechanical properties under solicitations. The effect of shearing was not investigated.

In our experimental conditions, as the tribofilms generated with both additives are made of phosphate materials, same kind of anti-wear mechanisms can be proposed for both molecules. The tribochemical reaction of polyphosphate with native iron oxide could explain the adhesion of the tribofilm on the substrate and the loss of abrasive character of wear particles. Although our experiments do

not allow any conclusion about structural changes during the tribological solicitations, same kind of modifications are expected for **ZP** and **ZDDP** tribofilms. Concerning extreme pressure conditions, no **ZP** activity is expected as there is no sulphur in the molecule.

At 25 °C and 25 mm/s for 360 m of sliding, tribological tests results show that **ZP** molecule exhibits a better anti-wear behaviour than **ZDDP**. At lower concentration (200 ppm of phosphorus—25 °C—25 mm/s—240 min), **ZP** additive shows an even better anti-wear behaviour than **ZDDP**. As it was proposed first (§1), the **ZP** molecule is closed in composition to tribofilm final material, so **ZP** molecule does not need to follow the thermo-oxidative degradation pathway of **ZDDP** molecule, avoiding high wear rate during the detrimental induction period of **ZDDP**. This makes the **ZP** molecule more reactive and more efficient than **ZDDP** at 25 °C, 25 mm/s and 360 m of sliding.

To conclude, **ZP** molecule has an advantage compared to **ZDDP** in terms of anti-wear capabilities at 25 °C. At 100 °C, it is **ZDDP** molecule that exhibits a better anti-wear behaviour. A mixture of both molecules is so an interesting option to get a good compromise in terms of anti-wear capabilities in the range of 25 and 100 °C with the same amount of phosphorus and with a small amount of sulphur atoms in the lubricant.

5 Conclusion

The comparison of **ZP** anti-wear performance with **ZDDP** allows us to conclude that

- although the anti-wear efficiency of these two molecules is found at 100 mm/s of sliding speed and 100 °C, **ZDDP** exhibits a slightly better anti-wear behaviour than **ZP** at this temperature. For both additives, tribofilms are mainly made of zinc and iron phosphate.
- at room temperature and 25 mm/s of sliding speed, **ZP** is a better anti-wear additive
- at room temperature and 25 mm/s of sliding speed, **ZP** is able to protect steel surfaces from wear even at 200 ppm of phosphorus. In these conditions, **ZDDP** is not so active.

Taking into account all these data, we show that **ZP** is an interesting anti-wear additive for the lubrication of Internal Combustion Engines at ambient temperature, which is the characteristic of cold engine start. In steady-state conditions, **ZDDP** molecule is more efficient than **ZP**. The combination of both additives (keeping a small amount of P) is a good option to optimise the anti-wear capabilities of engine lubricants. The efficiency of these additives in the EP regime was not studied. However, the loss of extreme pressure properties and antioxidant properties with **ZP** molecule is expected and requires the addition of other molecules in the lubricant completely formulated.

Acknowledgments The authors would like to thank the ANR for the support in the ANR-07-JCJC-0060 LOWPOLUB project.

References

1. Tannous, J., Dassenoy, F., Bruhacs, A., Tremel, W.: Synthesis and tribological performance of novel $Mo_xW_{1-x}S_2$ ($0 \leq x \leq 1$) inorganic fullerenes. Tribol. Lett. **37**, 83–92 (2010)
2. Martin, J.M., Ohmae, a.N.: Carbon-Based Nanolubricants. Tribology in Practice Series. Wiley, New Jersey (2008)
3. Mourhatch, R., Aswath, P.B.: Tribological behavior and nature of tribofilms generated from fluorinated ZDDP in comparison to ZDDP under extreme pressure conditions—Part 1: structure and chemistry of tribofilms. Tribol. Int. **44**, 187–200 (2010). In Press
4. Huq, M.Z., Aswath, P.B., Elsenbaumer, R.L.: TEM studies of anti-wear films/wear particles generated under boundary conditions lubrication. Tribol. Int. **40**, 111–116 (2007)
5. Gauvin, M., Dassenoy, F., Belin, M., Minfray, C., Guerret-Piécourt, C., Bec, S., Martin, J., Montagnac, G., Reynard, B.: Boundary lubrication by pure crystalline zinc orthophosphate powder in oil. Tribol. Lett. **31**, 139–148 (2008)
6. Spikes, H.: Low- and zero-sulphated ash, phosphorus and sulphur anti-wear additives for engine oils. Lubr. Sci. **20**, 103–136 (2008)
7. Spikes, H.: The history and mechanisms of ZDDP. Tribol. Lett. **17**, 469–489 (2004)
8. Fuller, M.L., Kasrai, S.M., Bancroft, G.M., Fyfe, K., Tan, K.H.: Solution decomposition of zinc dialkyldithiophosphate and its effect on anti-wear and thermal film formation studied by X-ray absorption spectroscopy. Tribol. Int. **31**, 627–644 (1998)
9. Rowe, C.N., Dickert, J.J.: The thermal decomposition of metal O, Odialkylphosphorodithioates. J. Org. Chem. **32**, 647–653 (1967)
10. Spedding, H., Watkins, R.C.: The anti-wear mechanisms of ZDDP's part I and part II. Tribol. Int. **15**, 9–15 (1982)
11. Mitchell, P.C.H.: Oil-soluble MO-S compounds as lubricant additives. Wear **100**, 281–300 (1984)
12. Martin, J.M.: Anti-wear mechanisms of zinc dithiophosphate: a chemical hardness approach. Tribol. Lett. **6**, 1–8 (1999)
13. Barnes, A.M., Bartle, K.D., Thibon, V.R.A.: A review of zinc dialkyldithiophosphates (ZDDPS): characterisation and role in the lubricating oil. Tribol. Int. **34**, 389–395 (2001)
14. Sheasby, J.S., Caughlin, T.A., Habeeb, J.J.: Observation of the anti-wear activity of zinc dialkyldithiophosphate additives. Wear **150**, 247–257 (1991)
15. Minfray, C., Le Mogne, T., Martin, J.-M., Onodera, T., Nara, S., Takahashi, S., Tsuboi, H., Koyama, M., Endou, A., Takaba, H., Kubo, M., Del Carpio, C.A., Miyamoto, A.: Experimental and molecular dynamics simulations of tribochemical reactions with ZDDP: zinc phosphate-iron oxide reaction. Tribol Trans **51**, 589–601 (2008)
16. De Barros, M.I., Bouchet, J., Raoult, I., Le Mogne, T., Martin, J.M., Kasrai, M., Yamada, Y.: Friction reduction by metal sulfides in boundary lubrication studied by XPS and XANES analyses. Wear **254**, 863–870 (2003)
17. Minfray,C., Martin, J. M., Esnouf, C., Le Mogne, T., Kersting, R., Hagenhoff, B.: A multi-technique approach of tribofilm characterisation. Thin Solid Films **447–448**, 272–277 (2004)
18. Rossi, A., Eglin, M., Piras, F., Matsumoto, M., Spencer, K.N.D.: Surface analytical studies of surface-additive interactions, by means of in situ and combinatorial approaches. Wear **256**, 578–584 (2004)

19. Minfray, C., Mogne, T., Lubrecht, A.A., Martin, J.-M.: Experimental simulation of chemical reactions between ZDDP tribofilms and steel surfaces during friction processes. Tribol. Lett. **21**, 65–76 (2006)
20. Yin, Z., Kasrai, M., Fuller, M., Bancroft, G., Fyfe, M.K., Tan, K.H.: Application of soft X-ray absorption spectroscopy in chemical characterization of anti-wear films generated by ZDDP part I: the effects of physical parameters. Wear **202**, 172–191 (1997)
21. Zhou, J.G., Thompson, J., Cutler, J., Blyth, R., Kasrai, M., Bancroft, G.M., Yamaguchi, E.S.: Resolving the chemical variation of phosphates in thin ZDDP tribofilms by x-ray photoelectron spectroscopy using synchrotron radiation: evidence for ultraphosphates and organic phosphates. Tribol. Lett. **39**, 101–107 (2010)
22. Gauvin, M.: Approche analytique in situ du mécanisme anti-usure des phosphates de zinc. Génie des matériaux. Ecole Centrale de Lyon, Lyon (2008)
23. Gauvin, M., Dassenoy, F., Minfray, C., Martin, J.M., Montagnac, G.: Reynard: zinc phosphate chain length study under high hydrostatic pressure by Raman spectroscopy. J. Appl. Phys. **101**, 063505 (2007)
24. Mosey, N.J., Müser, M.H., Woo, T.K.: Molecular mechanisms for the functionality of lubricant additives. Science **307**, 1612–1615 (2005)
25. Shakhvorostov, D., Müser, M.H., Song, Y., Norton, P.R.: Smart materials behavior in phosphates: role of hydroxyl groups and relevance to anti-wear films. J. Chem. Phys. **131**, 044704 (2009)
26. Shakhvorostov, D., Nicholls, M.A., Norton, P.R., Müser, M.H.: Mechanical properties of zinc and calcium phosphates: structural insights and relevance to anti-wear functionality. Eur. Phys. J. B **76**, 347–352 (2010)
27. Crobu, M., Rossi, A., Mangolini, F., Spencer, N.: Tribochemistry of bulk zinc metaphosphate glasses. Tribol. Lett. **39**, 121–134 (2010)
28. Kazuhiro Yagishita, J. I.: Long drain/fuel efficient engine oils based on the ZDDP substitute additive technology. SAE Int. **20030320** (2003-01-2003), 19–22 (2003)
29. Guibert, M., Nauleau, B., Kapsa, P., Rigaud, E.: Design and manufacturing of reciprocating linear tribometer. Journée Francophones de Tribologie: Tribologie et Couplages Multi-physique, Lille. Presse Polytechniques et Universitaires Romandes (2006)
30. Hamrock, B.J., Dowson, D.: Isothermal Elastohydrodynamic lubrication of point contacts part 1: theorical formulation. ASME J. Lubr. Tech. **98**, 223–229 (1976)
31. Walton J., P.W., Fairley, N., Carrick, A.: Peak Fitting with CasaXPS, vol Acolyte Science, Kinderton Close, High Legh, Knutsford, Cheshire, WA16 6LZ U.K, (2010)
32. Morina, A., Neville, A., Priest, M., Green, J.H.: ZDDP and MoDTC interactions in boundary lubrication—The effect of temperature and ZDDP/MoDTC ratio. Tribol. Int. **39**, 1545–1557 (2006)